



# CHORUS

This is the accepted manuscript made available via CHORUS. The article has been published as:

## CO Oxidation Facilitated by Robust Surface States on Au-Covered Topological Insulators

Hua Chen, Wenguang Zhu, Di Xiao, and Zhenyu Zhang

Phys. Rev. Lett. **107**, 056804 — Published 28 July 2011

DOI: [10.1103/PhysRevLett.107.056804](https://doi.org/10.1103/PhysRevLett.107.056804)

# CO Oxidation Facilitated by Robust Surface States on Au-Covered Topological Insulators

Hua Chen,<sup>1</sup> Wenguang Zhu,<sup>1,2</sup> Di Xiao,<sup>2</sup> and Zhenyu Zhang<sup>3,1</sup>

<sup>1</sup>*Department of Physics and Astronomy, University of Tennessee, Knoxville, TN 37996, USA*

<sup>2</sup>*Materials Science and Technology Division, Oak Ridge National Laboratory, Oak Ridge, TN 37831, USA*

<sup>3</sup>*ICQD/HFNL, University of Science and Technology of China, Hefei, Anhui, 230026, China*

Surface states—the electronic states emerging as a solid material terminates at a surface—are usually vulnerable to contaminations and defects. The robust topological surface state(s) (TSS) on the three-dimensional topological insulators provide a perfect platform for exploiting surface states in less stringent environments. Employing first-principles density functional theory calculations, we demonstrate that the TSS can play a vital role in facilitating surface reactions by serving as an effective electron bath. We use CO oxidation on gold-covered Bi<sub>2</sub>Se<sub>3</sub> as a prototype example, and show that the robust TSS can significantly enhance the adsorption energy of both CO and O<sub>2</sub> molecules, by promoting different directions of static electron transfer. The concept of TSS as an electron bath may lead to new design principles beyond the conventional *d*-band theory of heterogeneous catalysis.

PACS numbers: 73.20.-r, 82.65.+r, 68.43.-h

Surface states [1, 2] can be present in many systems, e.g., the free-electron like states on the (111) surfaces of noble metals [3], and the dangling bond derived states on semiconductor surfaces [4]. Aside from their spatial proximity, the *sp*- or *d*-band derived surface states can be located at or near the Fermi level ( $E_F$ ) in energy space; consequently they can significantly influence the physical and chemical processes happening at the surfaces [5–8]. However, since they arise as a result of the different bonding environment at the surface from the bulk [1], normal surface states are easily destroyed by local modifications at the surfaces, e.g., presence of impurities, surface defects, surface reconstruction, or a change in the surface termination or orientation. This fundamental limitation has prohibited systematic studies of the potential role of surface states in surface reactions and catalysis, especially in more realistic environments.

In contrast, the exotic metallic TSS of the recently discovered three-dimensional topological insulators (3DTI) [9–12] are exceptionally robust compared to conventional surface states. The TSS arise from the non-trivial topology of the electron bands of the 3DTI, and their persistence is protected by time-reversal symmetry. Therefore, the TSS are insensitive to the structural details of the surface [13, 14], and will persist as long as the bulk band gap embodying the TSS remains open. The robust TSS thus provides a perfect platform for investigating the catalytic role of surface states in less constrained environments.

In our study, we focus on CO oxidation by supported Au films, a prototype system of fundamental and practical importance in heterogeneous catalysis [15–18]. The use of the 3DTI Bi<sub>2</sub>Se<sub>3</sub> [19, 20] as the substrate, instead of conventional oxides such as TiO<sub>2</sub> or MgO, is to introduce additional surface electron states (the TSS) at  $E_F$ . As shown recently for the case of metal-induced semi-

conductor surface reconstruction [21], such extra states may serve as an electron bath to significantly modify the bonding configurations on the surface through proper static electron transfer.

Our density functional calculations are carried out using the Vienna *ab initio* simulation package (VASP) [22] with PAW potentials [23, 24] and the generalized gradient approximation (PBE-GGA) [25] for exchange-correlation functional. The lattice constants of Bi<sub>2</sub>Se<sub>3</sub> are adopted from experiments. The generic Bi<sub>2</sub>Se<sub>3</sub> substrate is modeled by a slab of 15 atomic layers or 3 quintuple layers (QL), and a Bi-terminated substrate is realized by removing one outermost Se layer. The vacuum layers are over 20 Å thick to ensure decoupling between neighboring slabs. During relaxation, atoms in the lower 11 atomic layers are fixed in their respective bulk positions, and all the other atoms are allowed to relax until the forces on them are smaller than 0.01 eV/Å. A 7×7×1 *k*-point mesh is used for the 1×1 surface unit cell, and 3×3×1 for the 2×2 surface unit cell [26].

Crystalline Bi<sub>2</sub>Se<sub>3</sub> has rhombohedral structure and its unit cell is composed of 3 weakly coupled QL, each of which comprises of 5 alternating Bi and Se layers in a sequence Se-Bi-Se-Bi-Se [19, 20]. The naturally cleaved surface is therefore the Se surface. In Fig. 1 (a) we plot the band structure around  $E_F$  of a naturally cleaved 3 QL Bi<sub>2</sub>Se<sub>3</sub> film. The surface states in the bulk band gap ( $\sim 0.3$  eV) have close to linear dispersion near  $E_F$ . This single “Dirac-cone” like band structure is a distinctive feature of the TSS of Bi<sub>2</sub>Se<sub>3</sub> [19, 20]. The small gap ( $\sim 50$  meV) opened at the Dirac point is due to the coupling between the two degenerate TSS on the two surfaces of a very thin 3DTI film [27].

We use the Bi-terminated surface of Bi<sub>2</sub>Se<sub>3</sub>, to which Au binds more strongly than the naturally cleaved Se surface [28], to support Au atoms without formation of

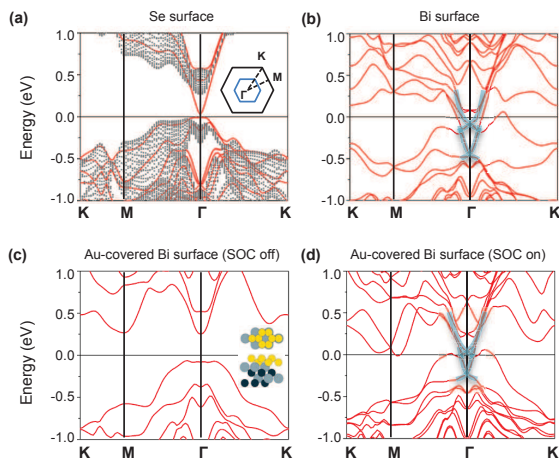


FIG. 1: (color online). (a) Band structure of a 3 QL  $\text{Bi}_2\text{Se}_3$  film, where the shaded area is the bulk band structure projected to the 2D Brillouin zone. The inset shows the shape of the 2D Brillouin zone for different surface unit cells (Black solid lines- $1\times 1$ ; blue solid lines- $2\times 2$ ). (b) Band structure of a Bi-terminated  $\text{Bi}_2\text{Se}_3$  film. (c) and (d) Band structures of 2 ML Au deposited on the Bi-terminated surface without and with SOC, respectively. In (b) and (d) the TSS are highlighted by the transparent blue lines. The inset in (c) shows the top and side views of the structure (only top 4 atomic layers of  $\text{Bi}_2\text{Se}_3$  are shown). Yellow balls-Au; light blue balls-Bi; dark blue balls-Se.

3D Au clusters [17]. Experimentally it is possible to intentionally introduce a large amount of Se vacancies on the surfaces of  $\text{Bi}_2\text{Se}_3$  or eventually form a complete Bi-terminated surface, due to the large vapor pressure difference between Bi and Se [27]. We therefore can use the ideal Bi-terminated surface in the present proof-of-principle study. The band structure of the Bi-terminated film is shown in Fig. 1 (b). The two TSS Dirac bands still robustly persist and shift below  $E_F$ , agreeing with experiments [13, 19]. Additionally, the degeneracy of the two Dirac bands is lifted, of which the upper and lower bands correspond to the TSS at the upper (Bi-terminated) and lower (Se-terminated) surface, respectively.

We choose 2 monolayers (ML) of Au deposited on the Bi surface of the  $\text{Bi}_2\text{Se}_3$  film (Fig. 1 (c) inset) as a model system because of its optimal stability [28] for subsequent calculations. Here 1 ML is defined to be the same number of atoms as that in each atomic layer of  $\text{Bi}_2\text{Se}_3$ , which is equal to 0.48 times the atom density in a (111) layer of bulk Au. Figs. 1 (c) and (d) show the band structures of the Au-covered  $\text{Bi}_2\text{Se}_3$  film without and with spin-orbit coupling (SOC), respectively. Two TSS Dirac bands emerge only when the SOC is switched on, confirming that the TSS indeed originates from the SOC of the bulk states [9, 10]. This observation allows us to conveniently isolate the effects of the TSS by comparative studies with and without SOC. The shape of the two

TSS bands near the  $\Gamma$  point closely resembles that of the TSS in Fig. 1 (b) for the Bi-terminated  $\text{Bi}_2\text{Se}_3$  film despite the slight shift in their relative positions in energy. Therefore the TSS survives even if the  $\text{Bi}_2\text{Se}_3$  surface is completely buried under the 2 ML Au film.

The CO binding energies on the model system with and without SOC, calculated as  $\Delta E = E_{\text{adsorbate}+\text{substrate}} - E_{\text{adsorbate}} - E_{\text{substrate}}$ , are listed in Table I. With SOC, the binding energy is considerably enhanced by 0.2 eV compared to that without SOC, accompanied by a decrease of the C-Au bond length from 2.029 Å to 1.981 Å. The enhanced CO binding with SOC is due to the static electron transfer facilitated by the TSS. To see this effect we first compare the local density of states (LDOS) on the C atom of an adsorbed CO with and without SOC, shown in Fig. 2 (a). The antibonding  $2\pi^*$  states shift to higher energies with SOC, indicating decreased electron occupation, and hence enhanced CO-Au binding [29, 30]. On the other hand, from Fig. 2 (c), the top Dirac band, corresponding to the TSS on the Au-deposited Bi-terminated surface, shifts to lower energy after the adsorption of CO, indicating increased electron occupation. Taken together, net electrons are transferred to the TSS serving as an electron bath when CO is adsorbed on the surface.

TABLE I: Binding energies (in eV) of CO and  $\text{O}_2$  on three comparative substrates. (1) 2 ML Au on Bi-terminated  $\text{Bi}_2\text{Se}_3$ , (2) freestanding 2 ML Au fixed in the same geometry as in (1), and (3) (unreconstructed) Au(111) surface. The CO/ $\text{O}_2$  coverage is 1/4 ML in (1) and (2), and 1/16 ML in (3). The geometries of adsorbed CO and  $\text{O}_2$  are shown in Figs. 2 (e) and (f), respectively.

		(1) Au- $\text{Bi}_2\text{Se}_3$	(2) 2 ML Au	(3) Au(111)
CO	SOC	0.49	0.95	0.30
	No SOC	0.29	0.92	0.27
$\text{O}_2$	SOC	0.23	0.52	<0.01
	No SOC	0.07	0.49	<0.01

The enhanced CO binding with SOC is not due to Au, though Au does have large SOC. To see this we consider two comparative cases: One is fixing the 2 ML Au film in vacuum with the  $\text{Bi}_2\text{Se}_3$  substrate removed; the other is the unreconstructed Au(111) surface. The Au(111) surface is modeled by a 4 layer slab, each layer comprising of 16 Au atoms, with the lower 2 layers fixed. From Table I, the CO binding energy differences with and without SOC are about one order of magnitude smaller ( $\sim 0.03$  eV) in these two latter cases. We also note that with SOC the CO binding energy on the Au- $\text{Bi}_2\text{Se}_3$  system is much larger than that on Au(111). Based on these results, we conclude that the TSS of the underlying  $\text{Bi}_2\text{Se}_3$  enhance the CO binding by accepting the electrons that otherwise would have been transferred to the antibonding states of the CO-Au system.

Next we show that the TSS as an electron bath can

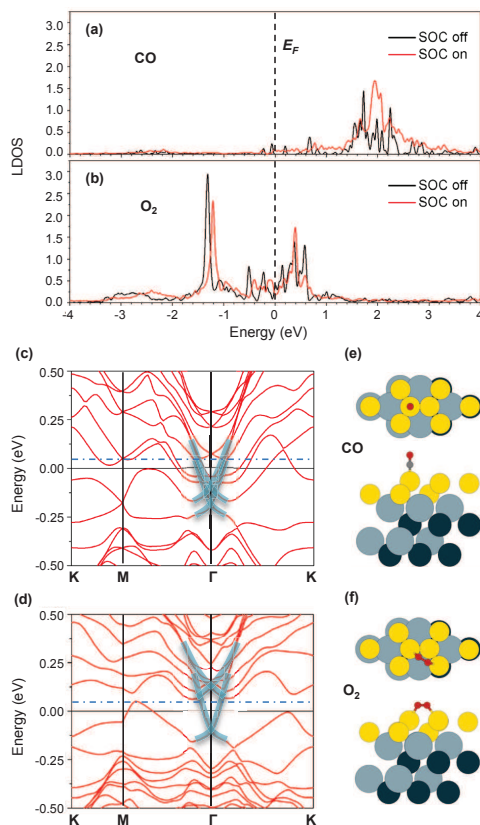


FIG. 2: (color online). (a) and (b) LDOS on the C atom of CO, and one O atom of O<sub>2</sub>, featuring the energy range corresponding to the 2π\* states of CO and O<sub>2</sub>, respectively. (c) and (d) Band structures of the CO and O<sub>2</sub> adsorbed 2 ML Au-Bi<sub>2</sub>Se<sub>3</sub> film, shown in a reduced Brillouin zone corresponding to the 2×2 surface unit cell (Fig. 1 (a) inset). The TSS bands are highlighted by the transparent blue lines. The blue dot-dash lines indicate the position of the upper Dirac point in Fig. 1 (d). The upper and lower panels in (e) and (f) are the top and side views of the atomic structures. Small red balls-O; small gray balls-C; yellow balls-Au; light blue balls-Bi; dark blue balls-Se.

also enhance the adsorption of O<sub>2</sub>, but by invoking a different direction of static electron transfer. On the Au-Bi<sub>2</sub>Se<sub>3</sub> substrate, O<sub>2</sub> binding energy increases by 0.16 eV with SOC, which is also much larger than that on the freestanding Au film or Au(111) surface (Table I). The LDOS on one O atom of O<sub>2</sub> is shown in Fig. 2 (b). The two groups of peaks below and above  $E_F$  correspond to the spin-up and spin-down antibonding 2π\* states, respectively [31]. As the half-filled 2π\* states hybridize with the Au *d* states, more electrons will be transferred to the 2π\* states and promote O<sub>2</sub> toward dissociation [31, 32]. At the same time, the spin splitting of the 2π\* states will decrease due to the weakened O-O bond. In Fig. 2 (b), both groups of the spin-split peaks shift toward  $E_F$  after turning on SOC, indicating

decreased spin splitting in the O<sub>2</sub> orbitals. Meanwhile, the O-O bond length increases from 1.289 Å without SOC to 1.299 Å with SOC. The increased electron occupation of the 2π\* states upon switching on SOC is not easily visible from Fig. 2 (b), but is confirmed by the calculated increase in the relative spectral weight of the 2π\* DOS below  $E_F$ , equal to 0.56 with SOC and 0.55 without SOC. This difference is roughly equal to 0.04 *e* per O<sub>2</sub> molecule, originated from the TSS. On the other hand, from Fig. 2 (d), the top TSS Dirac band shifts upward compared to that without O<sub>2</sub> adsorption, indicating that electrons are transferred out of the TSS. Therefore, rather than accepting electrons as in the case of CO, the TSS now donates electrons and promotes O<sub>2</sub> toward dissociative adsorption on Au. Moreover, the adsorption energy of O<sub>2</sub> is now comparable to that of CO with a moderate strength, which is a desirable feature for easier reaction and high catalytic activity.

In studying adsorption of molecules on transition metal surfaces, the prevailing theoretical framework has been the *d*-band theory, according to which the chemical activity of a metal substrate is correlated with the position of its *d*-band center ( $E_d$ ) in the energy spectrum [29, 30]. Specifically the closer  $E_d$  of the metal substrate to  $E_F$ , the stronger molecular adsorbates bind to the substrate. A major contribution to the energy gain as  $E_d$  shifts up toward  $E_F$  is from the decreased filling of the adsorbate’s antibonding states as they are “pushed away” from  $E_F$  by the *d* bands. To see whether our results can be explained independently by the *d*-band theory, we have calculated  $E_d$  of Au in the top layer of the 2 ML Au film [Figs. 3 (a) and (b)] as

$$E_d = \frac{\int_{-\infty}^{\infty} PDOS_d(E) \times (E - E_F) dE}{\int_{-\infty}^{\infty} PDOS_d(E) dE}, \quad (1)$$

where  $PDOS_d$  is the density of states projected to the *d* orbital of Au. We find that, in the present case,  $E_d$  actually shifts down away from  $E_F$  by 0.21 eV (from -2.68 eV to -2.89 eV) after switching on SOC, and the shift is even larger than that of the freestanding 2 ML Au film, which is 0.12 eV to the same direction (from -2.57 eV to -2.69 eV). These findings unambiguously rule out the *d*-band theory to be mainly operative in the present systems.

An implicit assumption of the *d*-band theory is that the *sp* states around  $E_F$  do not differ much among different systems. However, our present study offers a striking and unique counter example to this assumption. In particular, since these TSS are gapless and not completely filled, they can readily donate or accept electrons in order to lower the total energy upon molecular adsorption [see illustrations in Figs. 3 (c-e)]. Such *sp*-band derived states near  $E_F$ , either due to extrinsic effects such as the 3DTI substrate studied here or associated with the transition metals themselves, can play a prominent role

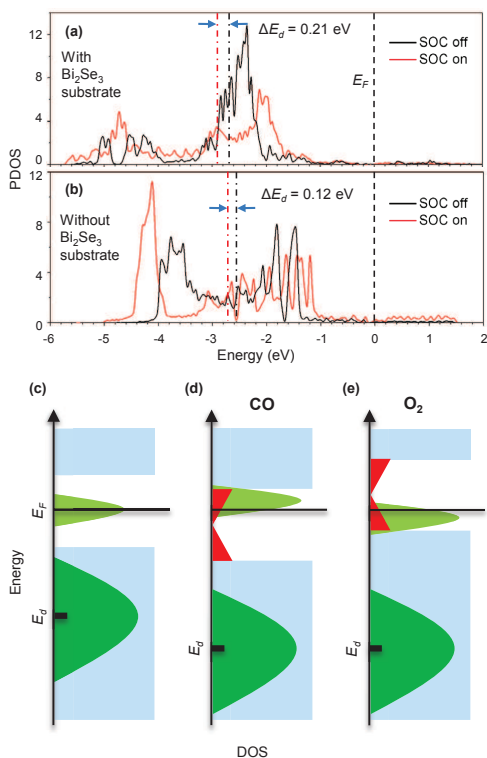


FIG. 3: (color online). (a) and (b) PDOS of an Au atom in the top layer of the 2 ML Au film with and without Bi<sub>2</sub>Se<sub>3</sub> substrate, respectively. In (b) the Au film is fixed in space. The red and black dot-dash lines indicate the positions of  $E_d$  with and without SOC, respectively. (c-e) Illustration of the role of the TSS in molecular adsorption. Blue-valence and conduction bands of the 3DTI support; light green-antibonding states of adsorbed molecules; red-TSS; dark green-metal  $d$  bands. (c) Without the TSS, the support will not be involved in the static electron transfer. (d) and (e) With the TSS, electrons of the molecule-metal system can be transferred either to or from the partially filled metallic surface states, depending on which way can lower the total energy.

in surface reactivity, especially for late transition metals with deeper  $d$  bands. Furthermore, the delocalized  $sp$  surface states may also help to smooth the energy profile of the surface and lower the diffusion and reaction barriers of the adsorbed molecules [5, 6], an intriguing aspect worth future investigations. The present study indicates manipulation of the  $sp$  surface states may be complementary to the guiding principles from  $d$ -band theory in searching and designing new catalysts, and 3DTI materials may offer rich opportunities for this purpose.

We thank Shunfang Li for helpful discussions. This work was supported by US National Science Foundation (Grant number 0906025), National Natural Science Foundation of China (Grant number 11034006), and the UT/ORNL Joint Institute for Advanced Materials (JIAM fellowship). DX was supported by the Division

of Materials Science and Engineering, Office of Basic Energy Sciences, US Department of Energy, The calculations were performed at National Energy Research Scientific Computing Center (NERSC) of US Department of Energy.

- [1] I. Tamm, Phys. Z. Sowjetunion **1**, 733 (1932).
- [2] W. Shockley, Phys. Rev. **56**, 317 (1939).
- [3] M. F. Crommie, C. P. Lutz, and E. M. Eigler, Nature **363**, 524 (1993).
- [4] G. V. Hansson and R. I. G. Uhrberg, Surf. Sci. Rep. **9**, 197 (1988).
- [5] E. Bertel, P. Roos, and J. Lehmann, Phys. Rev. B **52**, 14384(R) (1995).
- [6] N. Memmel and E. Bertel, Phys. Rev. Lett. **75**, 485 (1995).
- [7] A. Vojvodic, A. Hellman, C. Ruberto, and B. Lundqvist, Phys. Rev. Lett. **103**, 146103 (2009).
- [8] Z. Cheng *et al.*, Phys. Rev. Lett. **105**, 066104 (2010).
- [9] L. Fu, C. L. Kane, and E. J. Mele, Phys. Rev. Lett. **98**, 106803 (2007).
- [10] J. E. Moore and L. Balents, Phys. Rev. B **75**, 121306(R) (2007).
- [11] D. Hsieh *et al.*, Nature **452**, 970 (2008).
- [12] T. Zhang *et al.*, Phys. Rev. Lett. **103**, 266803 (2009).
- [13] D. Hsieh *et al.*, Nature **460**, 1101 (2009).
- [14] Y. L. Chen *et al.*, Science **325**, 178 (2009).
- [15] M. Haruta, Catal. Today **36**, 153 (1997).
- [16] M. S. Chen and D. W. Goodman, Science **306**, 252 (2004).
- [17] M. S. Chen and D. W. Goodman, Chem. Soc. Rev. **37**, 1860 (2008).
- [18] M. Bonn *et al.*, Science **285**, 1042 (1999).
- [19] Y. Xia *et al.*, Nature Phys. **5**, 398 (2009).
- [20] H. Zhang *et al.*, Nature Phys. **5**, 438 (2009).
- [21] L. X. Zhang, E. G. Wang, Q.-K. Xue, S. B. Zhang, and Z. Y. Zhang, Phys. Rev. Lett. **97**, 126103 (2006).
- [22] G. Kresse and J. Furthmüller, Phys. Rev. B **54**, 11169 (1996).
- [23] P. E. Blöchl, Phys. Rev. B **50**, 17953 (1994).
- [24] G. Kresse and D. Joubert, Phys. Rev. B **59**, 1758 (1999).
- [25] J. P. Perdew, K. Burke, and M. Ernzerhof, Phys. Rev. Lett. **77**, 3865 (1996).
- [26] M. Methfessel and A. Paxton, Phys. Rev. B **40**, 3616 (1989).
- [27] Y. Zhang *et al.*, Nature Phys. **6**, 584 (2010).
- [28] H. Chen, W. G. Zhu, D. Xiao, and Z. Y. Zhang, in preparation.
- [29] B. Hammer, Y. Morikawa, and J. K. Nørskov, Phys. Rev. Lett. **76**, 2141 (1996).
- [30] *Chemical Bonding at Surfaces and Interfaces*, edited by A. Nilsson, L. Pettersson, and J. K. Nørskov (Elsevier, Amsterdam, 2008).
- [31] B. Yoon, H. Häkkinen, and U. Landman, J. Phys. Chem. A **107**, 4066 (2003).
- [32] G. Mills, M. S. Gordon, and H. Metiu, J. Chem. Phys. **118**, 4198 (2003).